2026 IEEE/SICE International Symposium on System Integration (SII)
January 11-14, 2026. Cancún, México

Wearable Gravity Compensation System for Muscular Load Reduction in Manual Handling of Heavy Objects

Koki Ito*, Ryoma Koizumi, Ryuji Tsuzuki, Riku Shibahara, Ken'ichi Yano,
Department of Mechanical Engineering, Graduate School of Engineering, Mie University
*Corresponding Author: work@robot.mach.mie-u.ac.jp

***Abstract*— As the working population shrinks due to a decreasing birthrate and an aging society, greater workforce participation by women and the elderly is expected. However, the manual handling of heavy objects imposes significant physical burdens, limiting their involvement and worsening labor shortages. Conventional assistive devices support only specific body parts, leading to residual strain. In this study, a wearable weight offloading system was developed to reduce muscular load on both the lower back and the arms. Its effectiveness was demonstrated through lifting and carrying experiments with a 10 kg object.**

I. Introduction

In recent years, the declining birthrate and aging population have reduced the workforce, increasing expectations for women and elderly participation[1]–[5]. However, manual heavy-load handling causes significant strain and frequent accidents, making such work unsuitable for these groups and contributing to chronic labor shortages[6],[7]. The Ministry of Health, Labour and Welfare reports that lower back pain requiring four or more days of leave accounts for about 60 % of occupational injuries, while upper limb disorders from heavy loads are the most frequently compensated non-traumatic musculoskeletal disorders. In agriculture, delivery, and construction, unstable worksites and limited machinery access necessitate manual labor. Thus, a weight-offloading system that reduces physical burden in any work environment is urgently needed.

To date, numerous assistive devices have been developed and evaluated for labor support tasks[8]. Roveda et al. developed a lumbar exoskeleton optimized for lightweight, assemblability, and manufacturability using topology optimization[9]. Koopman et al. confirmed that the SPEXOR passive exoskeleton reduced lumbar compression force by up to 21 % during static forward bending and by an average of 14 % during lifting tasks[10]. Additionally, suppression of lumbar flexion suggested a reduced risk of tissue damage.

Musso et al. evaluated the effectiveness of an upper limb exoskeleton for preventing musculoskeletal disorders (MSDs) common in manufacturing and construction, confirming that shoulder flexor muscle activity decreased by up to approximately 45 % across all tasks[11]. Kong et al. designed a passive upper limb exoskeleton that significantly reduced muscle activity and discomfort during augmented reality tasks without compromising posture or performance[12]. These previously developed assistive devices have demonstrated the ability to reduce the activation of the erector spinae muscles. However, during tasks involving the transportation of heavy objects, a significant load is also placed on the arms, including the biceps brachii. Therefore, it is necessary to develop a device capable of reducing muscular load on both the lower back and the arms. In this study, we developed a wearable weight-offloading system that can reduce the muscular load on both the lower back and the arms during heavy object-handling tasks, such as transportation, vertical movement, and gripping. Specifically, we propose a device that reduces the lower back muscle load by transferring the object's load to the pelvis through a sub-Jacobian line support. In addition, by incorporating a gravity compensation mechanism using the spiral pulley developed by Tian et al.[13], the system mitigates the muscular load on the arms. Finally, we confirmed the effectiveness of our proposed system by conducting lifting and carrying experiments with a 10 kg object and comparing electromyographic signals during the tasks.

II. Wearable Weight Offloading System

A. Design of a Gravity Compensation Mechanism Using a Spiral Pulley

To implement a wearable weight offloading system with a sub-Jacobian line support device, a suspension mechanism that reduces arm load is essential. Some previously developed wearable support systems have used motorized suspension mechanisms to assist vertical load movement. However, incorporating large motors adds weight to the device, increasing the burden on the user.

Therefore, a miniaturized and lightweight version of the gravity compensation mechanism using a spiral pulley developed by Tian et al.[13] was applied to the proposed wearable weight offloading system. Fig. 1 shows a model of the gravity compensation mechanism using a spiral pulley.

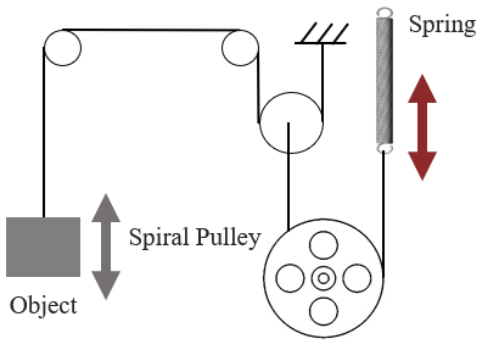

Figure 1. Model of the gravity compensation mechanism using a spiral pulley

The system in Fig. 1 maintains equilibrium at any height by balancing torque around the spiral pulley, with changes in the spiral radius compensating for spring extension or contraction during vertical object movement. As shown in Fig. 2, the spiral pulley includes a variable-radius spiral track and a constant-radius smooth pulley, creating a variable moment arm.

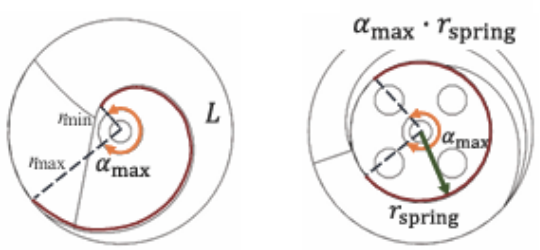

Figure 2. Spiral pulley geometry (left: spiral track side, right: smooth pulley side)

In the spiral pulley-based gravity compensation mechanism, the load displacement equals the pulley's rotation, as expressed in (1). Here, α_{max} is the maximum rotation angle, L is the spiral length, r_{spring} is the radius on the smooth pulley side, Δl_{max} is the spring's maximum extension, and L_{range} is the required motion range.

$$\alpha_{max}\, r_{spring} = \Delta l_{max} = L = L_{range} \tag{1}$$

Given the load mass m and its vertical movement range h, the load force F_{load} and required motion range L_{range} are calculated from (2) and (3); a suitable spring is then selected based on these values.

$$F_{load} = mg \tag{2}$$

$$L_{range} = h \tag{3}$$

The spring must be capable of compensating for the load calculated by (2) and must satisfy the required range of motion determined by (3). Therefore, (4) must hold to guarantee that these two requirements are simultaneously satisfied.

$$l_x \geq \Delta l_{max} + l_{initial} \tag{4}$$

Fig. 3 illustrates the force balance in cases in which the spiral track side of the spiral pulley is at its minimum radius and its maximum radius.

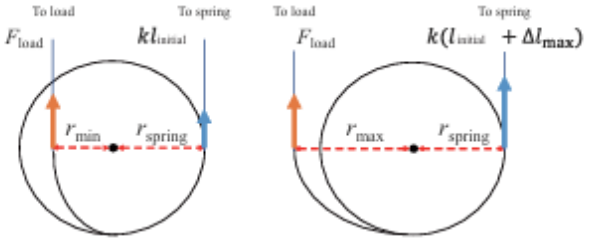

Figure 3. Force balance at minimum and maximum spiral radii

Based on Fig. 3, the condition for torque balance at the minimum spiral radius is given by (5). Here, r_{min} is the minimum spiral radius, $l_{initial}$ is the initial deflection of the spring, k is the spring constant, and r_{spring} is the radius of the smooth pulley.

$$F_{load} r_{min} = k l_{initial} r_{spring} \tag{5}$$

Since F_{load}, r_{min}, k and $l_{initial}$ are known values, the radius on the smooth pulley side of the spiral pulley, r_{spring}, can be obtained by solving (5) for r_{spring}.

Solving (1) for the maximum rotation angle α_{max} of the spiral pulley yields (6). Then, by substituting the radius of the smooth pulley side r_{spring} into (6), the maximum rotation angle α_{max} can be calculated.

$$\alpha_{max} = \frac{L_{range}}{r_{spring}} \tag{6}$$

Additionally, based on Fig. 2, the condition for torque balance at the maximum spiral radius is given by (7), where r_{max} is the maximum spiral radius

$$F_{load} r_{max} = k(\Delta l_{max} + l_{initial}) r_{spring} \tag{7}$$

By simultaneously solving (8) and (6) and eliminating $l_{initial}$, the maximum spiral radius r_{max} can be obtained using (8), thereby fixing the outer bound of the spiral trajectory.

$$r_{max} = r_{min} + \frac{k \Delta l_{max} r_{spring}}{F_{load}} \tag{8}$$

The spiral path of the spiral pulley is defined using the spiral equation given in (9) so that it becomes a quadratic function of the spiral pulley's rotation angle θ. Here, a, b, and c are design parameters.

$$r = a + b\theta + c\theta^2 \tag{9}$$

Since the spiral radius r becomes the minimum spiral radius when $\theta=0$ and the maximum spiral radius when $\theta=\alpha_{max}$, the constants a and b can be determined using (10).

$$\begin{cases} a = r_{min} \\ b = \dfrac{r_{max} - r_{min} - c\alpha_{max}^2}{\alpha_{max}} \end{cases} \tag{10}$$

Therefore, the spiral equation in (9) can be expressed using parameter c as shown in (11):

$$r = r_{min} + \frac{r_{max} - r_{min} - c\alpha_{max}}{\alpha_{max}} + c\theta^2 \tag{11}$$

Since the spiral length L can be written as a function of the spiral radius r by (12), we substitute the required motion range L_{range} for L and use (11) to express r. With these substitutions, the parameter c can be determined, thereby defining the spiral trajectory.

$$L = \int_0^{\alpha_{max}} r^2 + \left(\frac{\partial r}{\partial \theta}\right)^2 d\theta \tag{12}$$

B. THE WEARABLE WEIGHT OFFLOADING SYSTEM

A wearable weight offloading system was developed by integrating the sub-Jacobian line support device with a spiral pulley-based gravity compensation mechanism. Table I lists the specifications of the spiral pulley, and Fig. 4 shows the 3D-printed design based on those specifications.

TABLE I. Specifications of the spiral pulley

Thickness [mm]	64.0
Length of the spiral [mm]	140
Width of the groove [mm]	3.50
Maximum spiral radius [mm]	79.5
Minimum spiral radius [mm]	35.0
Normal pulley side radius [mm]	53.1
Maximum rotation angle [rad]	2.64

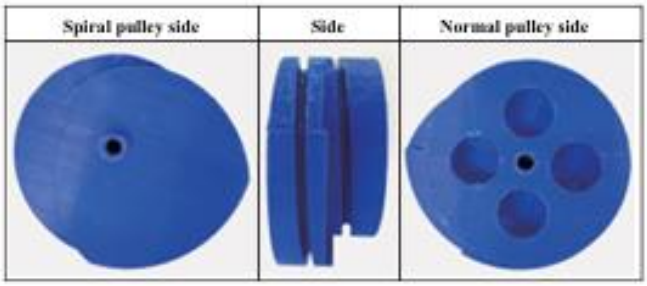

Figure 4. Designed spiral pulley

The spring selected for the gravity compensation mechanism was a tension coil spring with a small outer diameter that satisfies the specifications based on the load of the object and the required range of motion. The final developed wearable weight offloading system is shown in Fig. 5.

As shown in Fig. 5, the gravity compensation mechanism using spiral pulleys is mounted on both the left and right sides of the wearable weight offloading system. The suspension mechanism for the load was created by routing the wire connected to the spiral pulley through the pipe. Two guide pulleys are attached to the pipe to guide the wire and prevent it from derailing from the spiral pulley. The proposed system measures 500 mm in length, 400 mm in width, and 680 mm in height, and has a total weight of 4.7 kg.

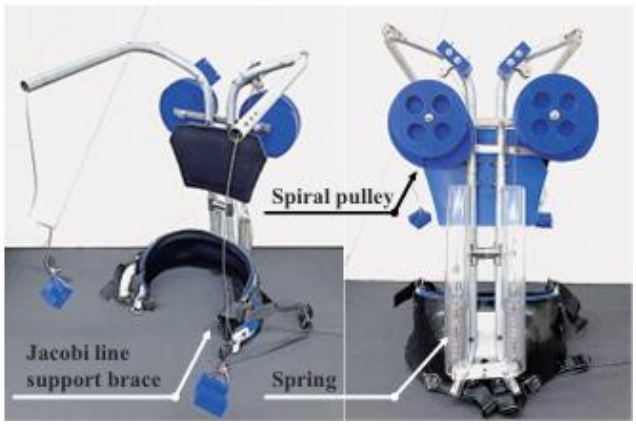

Figure 5. Wearable weight offloading system

III. VALIDATION EXPERIMENTS

To evaluate the wearable weight-offloading system, we conducted load-transportation and handling experiments. In the transportation task, six 10-kg loads were moved to targets at different heights while EMG from the erector spinae and biceps brachii was recorded.

The integrated EMG results with and without the system are shown in Figs. 6 and 7, respectively.

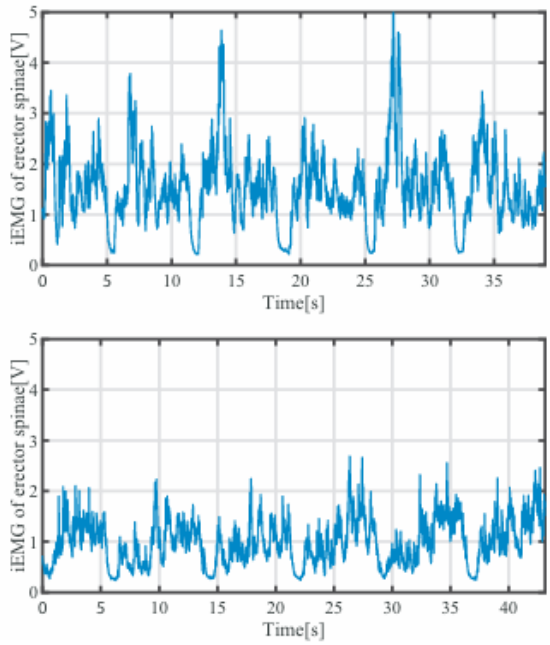

Figure 6. Integrated electromyographic activity of the erector spinae during transportation tasks with (lower panel) and without (upper panel) the proposed system

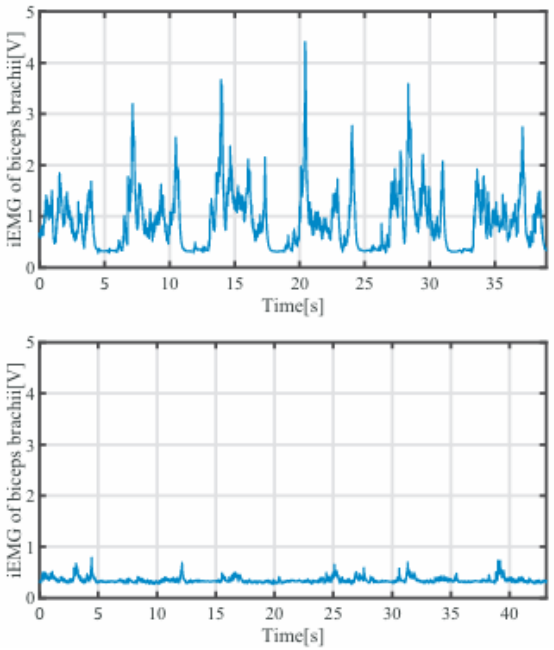

Figure 7. Integrated electromyographic activity of the biceps brachii during transportation tasks with (lower panel) and without (upper panel) the proposed system

Based on Figs. 6 and 7, use of the proposed system during 10 kg load transportation consistently reduced the integrated EMG activity of both the erector spinae and the biceps brachii compared with the no-device condition, across transport trials

at different target heights. On average, the integral EMG from task onset to completion decreased by 33% for the erector spinae and by 62% for the biceps brachii, indicating a marked reduction in back and upper-limb muscular demand while handling the load.

Next, as shown in Fig. 8, the subject performed upward and downward movements and holding tasks for four seconds each while holding a load, during which the EMG activity of the biceps brachii was measured using an EMG device. Fig. 9 shows the biceps brachii EMG activity with and without the proposed system during these tasks.

The data shown in Fig. 9 confirm that during heavy object handling tasks, the amplitude of the EMG activity decreases when the proposed system is used. Since an increase in EMG amplitude is known to correspond to increased muscle load, these results demonstrate that our proposed system can reduce the muscular burden on the biceps brachii.

Thus, our validation experiments confirmed that using the proposed system during heavy load tasks can reduce the muscular burden on both the erector spinae and the biceps brachii, demonstrating the effectiveness of our proposed system.

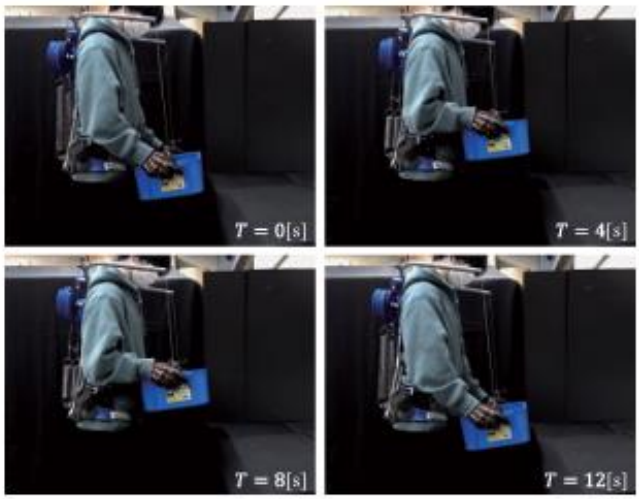

Figure 8. Handling tasks of heavy objects

IV. Conclusion

With labor shortages worsening due to a declining birthrate and an aging population, heavy load workplaces face challenges in mechanization, resulting in worker strain and injuries. Existing support devices assist only specific body parts, leaving residual muscular loads. To address this, we developed a wearable weight offloading system that supports loads below the Jacobian line to reduce the lumbar compressive force, and incorporates a spiral pulley-based gravity compensation mechanism. Its effectiveness was validated through lifting and transport experiments with heavy objects.

References

[1] R. R. Kato, "Population aging and labor mobility in Japan", Japan & The World Economy, vol. 62, 2022.

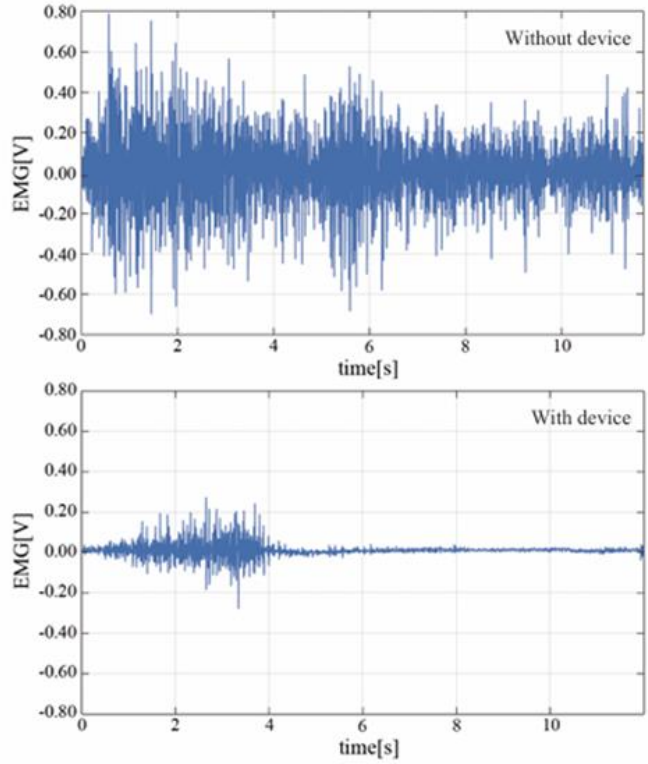

Figure 9. Handling tasks of heavy objects

[2] L. R. Halivni, B. Hovav, D. C. Christiani and S. B. Greenberg, "Aging workforce with reduced work capacity: From organizational challenges to successful accommodations sustaining productivity and well-being", Social Science & Medicine, vol. 312, 2022.

[3] A. Aitken and S. Singh, "Time to change? Promoting mobility at older ages to support longer working lives, The Journal of the Economics of Ageing, vol. 24, 2023.

[4] J. Banks, J. Gribb, G. Emmerson and D. Sturrock, "The impact of work on cognition and physical disability: Evidence from English women", Labour Economics, vol. 94, 2025.

[5] S. Kitao and M. Mikoshiba, "Females, the elderly, and also males: Demographic aging and macroeconomy in Japan", Journal of The Japanese and International Economies, vol. 56, 2020.

[6] E. Gakit and W. Karwowski, "Soft computing applications in the field of human factors and ergonomics: A review of the past decade of research", Applied Ergonomics, vol. 114, 2024.

[7] A. M. Shaikh, B. B. Mandal and S. M. Mangalavalli, "Causative and risk factors of musculoskeletal disorders among mine workers: Asystematic review and meta-analysis", Safety Science, vol. 155, 2022.

[8] Y. Zhou, J. Seo, Y. Gong, K. H. Heung, M. Khan and T. Lei, "Biomechanical assessment of a passive back exoskeleton using vision-based motion capture and virtual modeling", Automation in Construction, vol. 172, 2025

[9] L. Roveda, M. Pesenti, M. Rossi, M. C. Rodriguez, A. Pedrocchi, F. Braghin and M. Gandolla, "User-Centered Back-Support Exoskeleton: Design and Prototyping", Procedia CIRP, vol. 107, pp. 522-527, 2022.

[10] A. S. Koopman, M. Naf, S. J. Baltrusch, I. Kingma, C. R. Guerrero, J. Babic, M. P. Looze and J. H. Dieen, "Biomechanical evaluation of a new passive back support exoskeleton", Journal of Biomechanics, vol. 105, 2020.

[11] M. Musso, A. S. Oliveira and S. Bai, "Influence of an upper limb exoskeleton on muscle activity during various construction and manufacturing tasks", Applied Ergonomics, vol. 114, 2024.

[12] Y. K. Kong, S. S. Park, J. W. Shim, K. H. Choi, H. H. Shim, K. Kia and J. H. Kim, "A passive upper-limb exoskeleton reduced muscular loading during augmented reality interactions", Applied Ergonomics, vol. 109, 2023.

[13] S.Tian and K.Yano, "An innovative spiral pulley that optimizes cable tension variation for superior balancing performance", Journal of Robotics and Mechatronics, vol 34 no 3 pp 599 606 ,2022.